

Dispersion flattened photonic crystal fiber with high nonlinearity for supercontinuum generation at 1.55 μm

Long Zheng (郑龙), Xia Zhang (张霞)*, Xiaomin Ren (任晓敏), Huifang Ma (马会芳),
Lei Shi (施雷), Yamiao Wang (王亚苗), and Yongqing Huang (黄永清)

Key Laboratory of Information Photonics and Optical Communications, Ministry of Education, Institute of Optical Communications and Optoelectronics, Beijing University of Posts and Telecommunications, Beijing 100876, China

*Corresponding author: xzhang@bupt.edu.cn

Received September 9, 2010; accepted December 6, 2010; posted online March 28, 2011

A robust design for a photonic crystal fiber (PCF) based on pure silica with small normal dispersion and high nonlinear coefficient for its dual concentric core structure is presented. This design is suitable for flat broadband supercontinuum (SC) generation in the 1.55- μm region. The numerical results show that the nonlinear coefficient of the proposed eight-ring PCF is $33.8 \text{ W}^{-1}\cdot\text{km}^{-1}$ at 1550 nm. Ultraflat dispersion with a value between -1.65 and $-0.335 \text{ ps}/(\text{nm}\cdot\text{km})$ is obtained ranging from 1375 to 1625 nm. The 3-dB bandwidth of the SC is 125 nm (1496–1621 nm), with a fiber length of 80 m and a corresponding input peak power of 43.8 W. The amplitude noise is considered to be related to SC generation. For practical fabrication, the influence of the random imperfections of airhole diameters on dispersion and nonlinearity is discussed to verify the robustness of our design.

OCIS codes: 060.5295, 190.4370, 320.6629.

doi: 10.3788/COL201109.040601.

Broadband supercontinuum (SC) generation is attracting substantial research attention because of its enormous applications such as in optical coherence tomography (OCT)^[1], metrology^[2], optical sensing^[3], radio-over-fiber (ROF)^[4], and wavelength-division multiplexing (WDM) systems^[5,6]. In optical communications, both ROF and WDM systems work in the 1.55- μm waveband, so researchers focus on SC generation in this waveband. Spectrum width and flatness are considered as the two key parameters in evaluating the quality of SC spectrum. Low-amplitude noise is also important in achieving the required system performance. SC spectrum with a bandwidth of over 1000 nm has been reported. However, obtaining a relatively flat spectrum remains to be a challenge. To generate a flatly broadened SC, high nonlinearity and flat chromatic dispersion are essential. This requirement can be met by optimizing the design of the fiber and the pumping condition.

Photonic crystal fibers (PCFs) can engineer optical properties by designing the optical structure in cross-section, and the unique structure of PCFs can supply optimized dispersion and nonlinearity for better SC performance^[7–14]. Martin-Lopez *et al.*^[15] generated a spectrally bounded SC spanning 1550 to 1700 nm with a fiber which has two zero-dispersion wavelengths. Liao *et al.*^[16] generated a SC spectrum of 20-dB bandwidth spanning 800 to 2400 nm using a chalcogenide-tellurite composite microstructure fiber. Feng *et al.*^[17] generated a broad SC from 0.9 to 2.5 μm with a single-mode tellurite glass holey fiber. In all of these studies, pump pulses were operated in the anomalous dispersion region of the fiber, so the output SC spectra showed significant spectral oscillations (around 20 dB) which limited their telecommunication applications. One efficient way to avoid spectral fluctuations is to allow the pump pulses to work in the normal dispersion region. In our previous work, optical fiber with a small normal dispersion over

a wide wavelength region has been theoretically shown to be suitable for flat broadband SC generation. However, a specified structure of PCF was not proposed^[18]. In the experiment, the broadening width of SC was also achieved at 92 nm (at 6 dB) using PCF (made by Crystal Fiber, with the nonlinear coefficient at $11 \text{ W}^{-1}\cdot\text{km}^{-1}$)^[19].

In this letter, a PCF with small normal flat dispersion and high nonlinearity at the 1.55- μm region is designed using the finite difference (FD) beam propagation method (BPM) with transparent boundary conditions. The numerical results show that the proposed PCF is suitable for a flattened broadening and efficient SC generation (the 3-dB bandwidth is 125 nm), with a fiber length of 80 m and a corresponding pump power of 43.8 W. The amplitude noise related to SC generation is also discussed. In addition, the robustness of the design is taken into consideration.

A dual concentric core fiber aiming at normal dispersion and a high nonlinear coefficient, which is made of pure silica, is proposed. The x - y dimensional geometry of the proposed eight-ring PCF is shown in Fig. 1^[20]. The core of the proposed PCF is pure silica, and the cladding is formed by a triangular lattice of air holes. The air

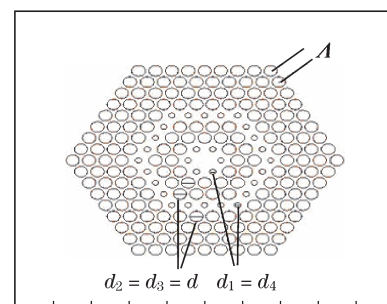


Fig. 1. Geometry of the proposed PCF.

hole pitch is labeled Λ as the distance between the centers of neighboring air holes. The two diameters for the air holes are d_1 and d_2 , respectively. The diameter for the first and fourth air holes is $d_1 = d_4$, and the other holes including the center core have the same diameter as $d_2 = d_3 = d$.

To investigate the propagation properties of PCF, BPM is utilized, which is a mode solver in commercial software (Rsoft Design Group, Ossining, New York) based on FD BPM. This method propagates a launched field profile along the longitudinal z axis of the PCF. The correlation function of the initial profile with the propagated profile at each point in the waveguide is constructed. The Fourier transformation of this correlation function extracts periodic variations, which determines the propagation constants and the effective indices $n_{\text{eff}}(\lambda)$ for the modes^[21]. The full transparent boundary condition is positioned outside the outermost ring of holes to reduce the simulation window^[22]. The simulation is performed in a window of 20×20 (μm) within the transverse x - y plane of the PCF, with step sizes of $\Delta z = 0.1$ μm , $\Delta x = \Delta y = 0.02$ μm . Meanwhile, the tolerance for $n_{\text{eff}}(\lambda)$ convergence is as low as 4×10^{-5} , which is an indication that the numerical precision of this modeling tool is reliable.

After the modal effect $n_{\text{eff}}(\lambda)$ was obtained by solving an eigenvalue problem drawn from Maxwell's equations using BPM, the mode dispersion parameter $D(\lambda)$, the confinement parameter L_c , and the effective area A_{eff} can easily be calculated^[23].

Dispersion leads directly to pulse broadening, walk-off, and phase-matching conditions, so it plays an important role in the performance of a nonlinear fiber, which in turn determines the bandwidth and power requirement of the device. For most telecommunication applications, a zero-dispersion magnitude and a small slope are necessary. The total dispersion $D(\lambda)$ in ps/(nm·km) of a PCF is obtained by summing up the waveguide dispersion and material dispersion:

$$D(\lambda) = D_w(\lambda) + D_m(\lambda), \quad (1)$$

$$D_w(\lambda) = -\frac{\lambda}{c} \frac{d^2 \text{Re}[n_{\text{eff}}]}{d\lambda^2}, \quad (2)$$

$$D_m(\lambda) = -\frac{\lambda}{c} \frac{d^2 n_m}{d\lambda^2}, \quad (3)$$

where $\text{Re}[n_{\text{eff}}]$ is the real part of the refractive index, λ is the operating wavelength, and c is the velocity of light in vacuum. Material dispersion $D_m(\lambda)$ can be calculated using the Sellmeier equation.

The nonlinearity is typically observed only at very high light intensities. The nonlinear coefficient in $\text{W}^{-1} \cdot \text{km}^{-1}$ is calculated by^[24]

$$\gamma = \frac{2\pi}{\lambda} \cdot \frac{n_2}{A_{\text{eff}}}, \quad (4)$$

where γ is the nonlinear coefficient, $n_2 = 2.6 \times 10^{-20}$ m^2/W is the nonlinear refractive index that is an indicator of the degree for nonlinear effects (four-wave mixing, stimulated Raman or Brillouin scattering) that will occur in a fiber with higher propagating power values, and $A_{\text{eff}} = \frac{(\int \int |\mathbf{E}|^2 dx dy)^2}{\int \int |\mathbf{E}|^4 dx dy}$ is the effective mode area

of the core area^[25], in which \mathbf{E} is the electric field of the medium. A small effective area provides the high-density power needed for significant nonlinear effects. The effective area can be directly related to the spot size, with the Gaussian width w and $A_{\text{eff}} = \pi w^2$ ^[25].

After the precise adjustment of the structure of PCF using different combinations of parameters, the best parameters by which a flat normal dispersion can be achieved are obtained, and the PCF is found to be suitable for flat broadband SC generation^[18].

Figure 2 represents the dispersion and nonlinearity curves of the proposed highly nonlinear (HNL) PCF. The optimal parameters are $d_1/\Lambda = d_4/\Lambda = 0.40$, $d_2/\Lambda = d_3/\Lambda = d/\Lambda = 0.82$, and $\Lambda = 0.87$ μm , and the ultra flattened dispersion between -1.65 and -0.335 ps/(nm·km) is obtained within the range of 1450 to 1650 nm, whereas the ring number is set as $N_r = 8$. All dispersion values in the parabola profile are under 0, indicating a small normal dispersion. Especially at the peak of the profile (1550 nm), the dispersion value is as low as -0.340 ps/(nm·km). With a larger wavelength, the nonlinearity decreases, but the nonlinearity values in the range of 1450 to 1650 nm are all higher than 30 $\text{W}^{-1} \cdot \text{km}^{-1}$, and at 1550 nm, the value of nonlinearity is as high as 33.8 $\text{W}^{-1} \cdot \text{km}^{-1}$. The values of dispersion and nonlinearity are suitable for the flat broadened SC.

The electric field distribution is demonstrated in Fig. 3, which represents the mode field intensity distribution of the fiber at 1550 nm wavelength corresponding to the optimal design. Figure 3 proves that the mode field has been confined well in the core. There is still no obvious light leakage into the cladding region beyond the first ring at other wavelengths as well as at 1550 nm, which is also observed and proven during the simulation.

The hole radius of the fiber is in submicron scale, so this presents a considerable challenge for present fabrication technology^[26-28]. Especially for a very small hole radius, the difference in radius among holes is large. The large hole has a diameter about two times that of the small hole. Another important issue to be considered for PCFs is the fabrication process^[29,30]. A high degree of fabrication accuracy is required for HNL PCF because a small change in dimension can cause some important properties to drift from the optimum value. Considering that there is no perfect fabrication for the designed PCFs, each air hole diameter is assumed to be obtained with Gaussian probability distribution, and the deviation is within 3% of the proposed value. Previous research

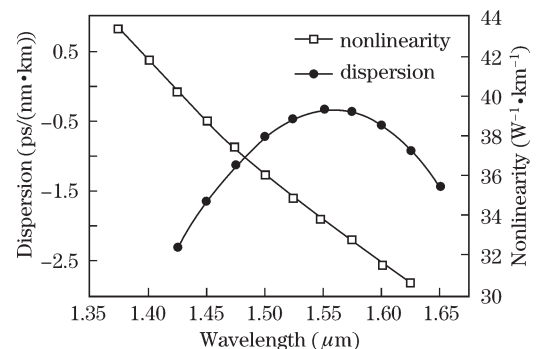


Fig. 2. Chromatic dispersion and nonlinearity value profile of the proposed PCF.

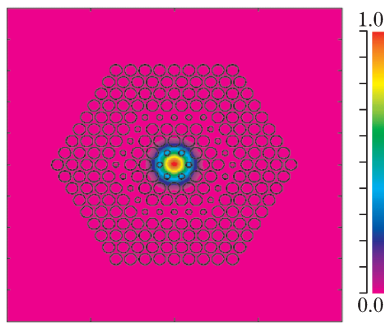


Fig. 3. Mode field pattern of the fundamental mode at 1550 nm.

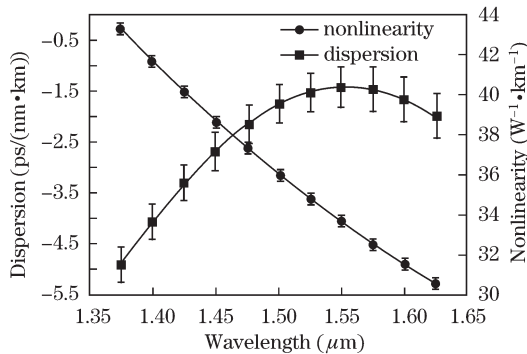


Fig. 4. Dispersion and nonlinearity of PCF for the 10 samples within 3% deviation of the optimum value.

indicated that this level of accuracy during fabrication was feasible^[31].

The fluctuations in the dispersion coefficients and nonlinearity of 10 PCF samples with irregular air hole diameters are shown in Fig. 4. The variation in air hole sizes results in a change in the effective index from that of a perfect structure, so the dispersion and nonlinearity curves are affected. The trend is the same as the proposed result. The mean values of the dispersion are all within the normal dispersion region (-4.90197--1.41008 ps/(nm·km)). The standard deviation $SD = \sqrt{\sum (x_i - \bar{x})^2 / (n - 1)}$ is below 1.30784, and the standard error for mean (SEM), $SEM = SD / \sqrt{n}$ is below 0.43595. Furthermore, these values increase when the wavelength becomes longer. Figure 4 shows that the nonlinear value is almost the same as the previous result. The SD is below 0.24485, and the SEM is below 0.08162. In addition, the fluctuations in the nonlinearity are so small, indicating that the fabrication error can hardly affect the performance of the proposed PCF. In other words, the PCF still has high nonlinearity and flattened dispersion. As a conclusion, the proposed structure is robust for imperfect fabrication.

To further understand the effect of pumping conditions on flat broadband SC generation, numerical simulations are conducted to examine SC generation in the proposed PCF. Pulse propagation in the fiber is modeled by solving the generalized nonlinear Schrödinger equation using the split-step Fourier method.

The propagation of the sech^2 waveform with full-width at half-maximum (FWHM), $T_{FWHM} = 1.6$ ps, is considered through the proposed PCF^[32]. The fiber parameters used in the simulation are given as $\gamma = 33.8$

$W^{-1} \cdot km^{-1}$, $\beta_2 = 0.4720$ ps²/km, $\beta_3 = 0.0033$ ps³/km, and $\beta_4 = -1.8123 \times 10^{-5}$ ps⁴/km at 1550 nm.

In a normal dispersion fiber, the spectral broadening is proportional to the soliton factor N which is defined as $N = (L_D / L_{NL})^{1/2}$, where L_D is the dispersion length, and L_{NL} is the nonlinear length. The dispersion length is defined as $L_D = T_0^2 / \beta_2$, where β_2 is the group velocity dispersion (GVD), and T_0 is the half width at 1/e intensity point; it is related to $T_{FWHM} = 1.763T_0$ for hyperbolicsecant pulse. The nonlinear length can be written as $L_{NL} = 1 / \gamma P_0$, and P_0 is the peak power of the pump pulse. Thus, N can be written as $(\gamma P_0 T_0^2 / \beta_2)^{1/2}$. For a given input pulse width, the spectral broadening can be enhanced by increasing the input power and using a SC fiber with a higher nonlinearity and smaller GVD.

Figure 5 shows the simulated output spectra from the 80-m-long SC fiber at different input power values. When the input peak power values are 5.5, 17.4, 21.9, and 43.8 W at a repetition rate of 10 GHz, the average input power values are 20, 25, 26, and 29 dBm, respectively, and the 3-dB bandwidth of the SCs is 25, 66, 79, and 125 nm, respectively. The spectral oscillations are significantly small. The spectrum is nearly symmetrically broadened with an increase in input power. Within an appropriate range, with a higher input power, a broader and flatter spectrum can be generated.

The most notable feature of the generated SC spectrum is that the spectral broadening is accompanied by an oscillatory structure covering the spectrum range. As can be seen clearly, the spectrum consists of many small peaks. These features show a typical pattern of self-phase modulation (SPM), which is assumed to be the dominant nonlinear effect responsible for the spectral broadening. The multipeak structure in the spectrum is a result of interference between the same optical frequencies in the pulse, and the relatively flat SC generation results from the combination effect of SPM and fiber normal dispersion. When the input power is lower, the oscillation in the spectrum is more significant, and the spectrum is far from being flat. With an increase in the input power, the oscillations gradually diminish, and the flat broadband SC is generated eventually.

The shot noise is modeled semiclassically by subdividing the original input electric field pulse into small time steps^[33]. This is followed by the addition of a variation (which obeys Gaussian distribution, and the mean square

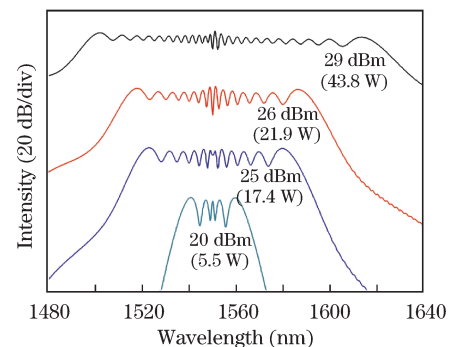


Fig. 5. Simulated output spectra from the proposed PCF for different input average power values of 20, 25, 26, and 29 dBm corresponding to peak power values of 5.5, 17.4, 21.9, and 43.8 W, respectively.

deviation is 1%) in the magnitude of the input pulse electric field in each time step. An equivalent frequency-domain implementation of the input pulse shot noise is found to yield identical results. These variations then propagate through the PCF and are generally amplified because of the nonlinear nature.

At a certain input power, for a given set of input parameters, a pulse train of 20 pulses is numerically generated using different random seeds for the input pulse shot noise in the propagation of each pulse along the proposed PCF. The mean spectral intensity can be calculated from all 20 pulses. The noise properties are quantified in terms of the relative intensity noise (RIN)^[33], which is defined as

$$\text{RIN} = \langle (\Delta P)^2 \rangle / (P_{\text{AVG}})^2, \quad (5)$$

where $(\Delta P)^2$ is the mean square intensity fluctuation spectral density of the optical signal, and P_{AVG} is the average optical power.

Figure 6(a) shows the relationship between RIN and wavelength for different input average power values. The level of input shot noise itself is -130 dBc/Hz. At average input powers of 20, 25, 26, and 29 dBm, the RIN mean values of the SCs are -97 , -85 , -82 , and -76 , respectively. In an appropriate range, as expected, with a higher input power, the RIN value increases. Meanwhile, the amplitude noise (%) is calculated, which can be described by the oscillation degree, defined as $\sqrt{\sum (P_i - \bar{P})^2 / (n - 1) / \bar{P}}$ ($i=1,2,\dots,20$). In Fig. 6(b), the amplitude noise (%) of SC generated in PCF is calculated to be within 2%, which means the amplitude noise is perfectly controlled during the propagation.

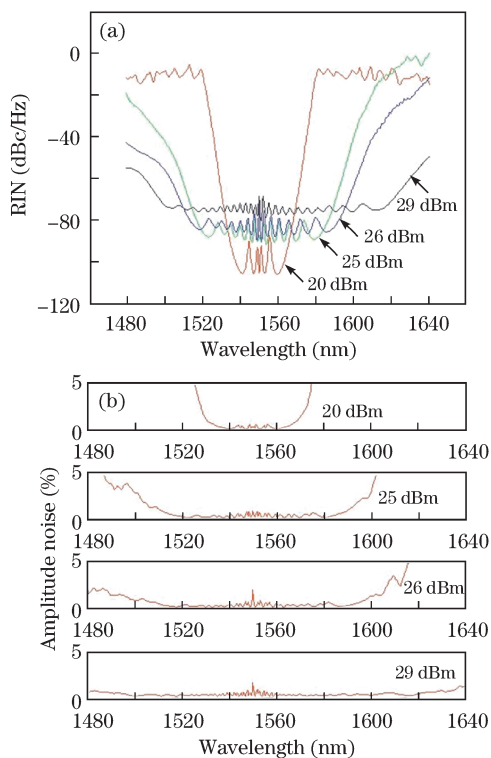


Fig. 6. (a) RINs and (b) amplitude noises for different input average power values of 20, 25, 26, and 29 dBm, respectively.

For the four different input power values mentioned above, the order of magnitude is comparable to the measured value of PCF in the experiment^[34].

In conclusion, a HNL PCF with small normal ultraflat chromatic dispersion has been proposed. By optimizing the geometrical parameters, dispersion is efficiently designed to be between -1.65 and -0.335 ps/(nm·km) within the range of 1450–1650 nm. The nonlinear value is greater than 33.8 W⁻¹·km⁻¹ at the telecommunication window of 1550 nm. This proposed PCF is suitable for a flattened broadening and efficient SC generation (the 3-dB bandwidth is 125 nm) in the 1.55- μ m region, with a fiber length of 80 m and a corresponding input peak power of 43.8 W. Finally, its tolerance for fabrication imperfections is also analyzed, and the results show that this structure is robust enough for practical applications such as in OCT, ROF, and WDM systems.

This work was supported by the National “973” Program of China (No. 2010CB327605), the National Natural Science Foundation of China (No. 61077049), the Program for New Century Excellent Talents in the University of China (No. NCET-08-0736), the Chinese Universities Scientific Fund (No. BUPT2009RC0410), and the National 111 Project of China (No. B07005).

References

1. I. Hartl, X. D. Li, C. Chudoba, R. K. Ghanta, T. H. Ko, J. G. Fujimoto, J. K. Ranka, and R. S. Windeler, *Opt. Lett.* **26**, 608 (2001).
2. K. Kim, B. R. Washburn, G. Wilpers, C. W. Oates, L. Hollberg, N. R. Newbury, S. A. Diddams, J. W. Nicholson, and M. F. Yan, *Opt. Lett.* **30**, 932 (2005).
3. H. Kano and H. Hamaguchi, *Opt. Lett.* **28**, 2360 (2003).
4. J. J. V. Olmos, T. Kuri, and K. Kitayama, *J. Lightwave Technol.* **25**, 3374 (2007).
5. T. Morioka, S. Kawanishi, K. Mori, and M. Saruwatari, *Electron. Lett.* **30**, 1166 (1994).
6. A. E. H. Oehler, S. C. Zeller, K. J. Weingarten, and U. Keller, *Opt. Lett.* **33**, 2158 (2008).
7. J. C. Knight, T. A. Birks, P. St. J. Russell, and D. M. Atkin, *Opt. Lett.* **21**, 1547 (1996).
8. P. Russel, *Science* **299**, 358 (2003).
9. J. M. Dudley and J. R. Taylor, *Supercontinuum Generation in Optical Fibers* (Cambridge University Press, Cambridge, 2010).
10. B. Dabas and R. K. Sinha, *Opt. Commun.* **283**, 1331 (2010).
11. Y. X. Jin, C. C. Chan, Y. F. Zhang, and X. Y. Dong, *Opt. Commun.* **283**, 1303 (2010).
12. L. Fang, J. Zhao, and X. Gan, *Chin. Opt. Lett.* **8**, 1028 (2010).
13. S. Wang, M. Hu, X. Fang, Y. Zhang, Y. Song, L. Chai, and Q. Wang, *Chinese J. Lasers (in Chinese)* **37(S1)**, 208 (2010).
14. T. Wang, H. Chen, S. Xie, B. Hraimel, L. Ma, and X. Zhang, *Chin. Opt. Lett.* **8**, 1037 (2010).
15. S. Martin-Lopez, L. Abrardi, P. Corredera, M. Go. Herraes, and A. Mussot, *Opt. Express* **16**, 6745 (2008).
16. M. Liao, C. Chaudhari, G. Qin, X. Yan, C. Kito, T. Suzuki, Y. Ohishi, M. Matsumoto, and T. Misumi, *Opt. Express* **17**, 21608 (2009).
17. X. Feng, W. H. Loh, J. C. Flanagan, A. Camerlingo, S. Dasgupta, P. Petropoulos, P. Horak, K. E. Frampton, N.

- M. White, J. H. Price, H. N. Rutt, and D. J. Richardson, *Opt. Express* **16**, 13651 (2008).
18. Y. Xu, X. Ren, X. Zhang, Y. Huang, and W. Xu, *Chin. Phys. Lett.* **22**, 1923 (2005).
19. Y. Xu, X. Ren, Z. Wang, X. Zhang, and Y. Huang, *Electron. Lett.* **43**, 87 (2007).
20. Y. Wang, X. Zhang, X. Ren, L. Zheng, X. Liu, and Y. Huang, *Appl. Opt.* **49**, 292 (2010).
21. G. R. Hadley, *IEEE J. Quantum Electron.* **28**, 363 (1992).
22. K. Kaneshima, Y. Namihira, N. Zou, H. Higa, and Y. Nagata, *IEICE Trans. Electron.* **E89-C**, 830 (2006).
23. F. Zolla, G. Renversez, A. Nicolet, B. Kuhlmeiy, S. Guenneau, and D. Felbacq, *Foundations of Photonic Crystal Fibres* (Imperial College Press, London, 2005).
24. G. Agrawal, *Nonlinear Fiber Optics, 2nd ed.* (Academic Press, San Diego, 1995).
25. N. A. Mortensen, *Opt. Express* **10**, 341 (2002).
26. M. Liao, X. Yan, G. Qin, C. Chaudhari, T. Suzuki, and Y. Ohishi, *Opt. Express* **17**, 15481 (2009).
27. T. M. Monro and H. Ebendorff-Heidepriem, *Annu. Rev. Mater. Res.* **36**, 467 (2006).
28. M. Liao, C. Chaudhari, G. Qin, X. Yan, T. Suzuki, and Y. Ohishi, *Opt. Express* **17**, 12174 (2009).
29. K. Reichenbach and C. Xu, *Opt. Express* **13**, 2799 (2005).
30. Z. Wang, X. Ren, X. Zhang, Y. Xu, and Y. Huang, *J. Opt. A: Pure Appl. Opt.* **9**, 435 (2007).
31. G. Zhou and L. Hou, in *Proceedings of the Doctoral Forum of China* 012 (2006).
32. Y. Xu, X. Ren, Z. Wang, X. Zhang, and Y. Huang, *Chin. Phys. Lett.* **24**, 734 (2007).
33. K. L. Corwin, N. R. Newbury, J. M. Dudley, S. Coen, S. A. Diddams, B. R. Washburn, K. Weber, and R. S. Windeler, *Appl. Phys. B* **77**, 269 (2003).
34. X. Sang, C. Yu, J. Ma, X. Xin, K. Wang, and Q. Zhang, *J. Optoelectron. Adv. Mate.* **3**, 85 (2009).